A BEM-based mathematical model of the human cornea stress-strain state

Cite as: AIP Conference Proceedings **2176**, 030001 (2019); https://doi.org/10.1063/1.5135125
Published Online: 19 November 2019

N. A. Babailov, A. E. Bogachev, S. A. Korotkih, et al.

A BEM-Based Mathematical Model of the Human Cornea Stress-Strain State

N. A. Babailov[1, a)], A. E. Bogachev[2, b)], S. A. Korotkih[2, c)], O. A. Nefedova[1, d)], and L. F. Spevak[1, e)]

[1]Institute of Engineering Science, Ural Branch of the Russian Academy of Sciences, 34 Komsomolskaya St., Ekaterinburg, 620049, Russia
[2]Ural State Medical University, 3 Repina St., Ekaterinburg, 620109, Russia

[a)]Corresponding author: fupi_vs@e1.ru
[b)]dr.a.bogachev@yandex.ru
[c)]bogach33@yandex.ru
[d)]nefedova@imach.uran.ru
[e)]lfs@imach.uran.ru

Abstract. The paper develops a mathematical model describing the behavior of the human cornea affected by intraocular pressure and external factors. The relevance of the study stems, particularly, from the urgent ophthalmological problems of hyperopia treatment. An effective remedy for hyperopia treatment is laser vision correction consisting in cornea deformation. The mathematical model enables the condition of the cornea after surgery to be estimated. The proposed model is based on the calculation of the cornea stress-strain state via the solution of a boundary value problem of elastostatics.

INTRODUCTION

The problem of mathematical modeling of the functioning of human organs is currently an inseparable part of the development of new methods for diagnosis, treatment, and prevention of numerous diseases. This paper proposes a mathematical model of the behavior of the human cornea, which may be applicable to the surgical treatment of hyperopia.

At present, prevention and treatment of abnormal eye refraction is an urgent ophthalmological problem. Hyperopia (farsightedness) is the most widespread deviation, found in 30 to 40% of the population in Russia [1]. The quality of vision in patients is largely affected by hyperopia of grades 2 and 3. In most cases, hyperopia is a congenital anomaly of refraction caused by antenatal eyeball underdevelopment or maldevelopment. At the same time, hyperopia below 3.0 D is a widespread and normal kind of refraction in early-year children, but its value decreases with age, up to complete disappearance due to eye growth [1, 2]. In many studies, the evaluated percentage of hyperopia above 2 D at the age under 5 fluctuates from 4 to 26%, and it ranges between 1 and 9% at the age above 15 [3–6]. Herewith, there is a further increase in the number of cases of hyperopia. According to the data provided by the National Eye Institute, USA, the number of cases of hyperopia increased by 16% between 2000 and 2010, and it is predicted to increase by 41% in 2030 as compared to 2000 [2]. Thus, hyperopia is a serious medical and social problem tending to become worse. Laser vision correction consisting in cornea deformation is the most effective medication for treating hyperopia. The mathematical model enables the cornea condition after surgery to be estimated.

The mathematical description of the cornea behavior is based on a model of elastic deformation and the stress-strain state (SSS) calculation procedure. Most of the so-far developed mathematical human eye models are based on the finite element method (FEM) and implemented in the ANSYS engineering analysis software package [7–12], the

Mechanics, Resource and Diagnostics of Materials and Structures (MRDMS-2019)
AIP Conf. Proc. 2176, 030001-1–030001-5; https://doi.org/10.1063/1.5135125
Published by AIP Publishing. 978-0-7354-1923-0/$30.00

cornea being generally represented by a spherical structure. The shell theory was used in [13, 14] to determine the cornea SSS. Earlier, we developed algorithms and programs for solving one-dimensional and plane problems of the elasticity and heat conduction by the boundary element method [15–20]. In solving plane problems, we used formulas for analytic integration of influence functions over the boundary elements [21], which considerably increases solution accuracy. Besides, a technology and program for solving the axisymmetric problem for Poisson's equation was developed [22], where analytic integration is inapplicable. The approach proposed in [22] is here extended to solving elastostatic problems.

BOUNDARY VALUE PROBLEM STATEMENT

The proposed model of cornea behavior is based on the calculation of the cornea stress-strain state by solving the static boundary value problem of the elasticity theory:

in the domain V,

$$\sigma_{ij,i} = 0, \tag{1}$$

$$\varepsilon_{ij} = \left(u_{i,j} + u_{j,i}\right)/2, \tag{2}$$

$$\sigma_{ij} = 2\mu\varepsilon_{ij} + \frac{2\mu\nu}{1-2\nu}\varepsilon\delta_{ij}; \tag{3}$$

on the inner cornea surface S_1, the intraocular pressure is given as

$$f_i = f_i^*; \tag{4}$$

on the outer cornea surface S_2 there is atmospheric pressure

$$f_i = 0; \tag{5}$$

on the cornea-sclera interface S_3, rigid attachment is specified as

$$u_i = 0. \tag{6}$$

Here, σ_{ij} is stress tensor components, $f_i = \sigma_{ij} n_j$ is surface stress vector components, u_i is displacement vector components, ε_{ij} is strain tensor components, $\varepsilon = \varepsilon_{ii}$, δ_{ij} is the Kronecker delta, μ and ν are elastic constants. The problem is considered in the axisymmetric statement, Fig. 1. The solution domain is $\overline{V}$, the generatrix of the domain V, which lies in the half-plane r^+z.

SOLUTION ALGORITHM

The solution of the problem (1) – (6) by the boundary element method in cylindrical coordinates reduces to the boundary integral equation for the boundary point $\xi \in \overline{S} = \overline{S}_1 \cup \overline{S}_2 \cup \overline{S}_3$ [23],

$$\frac{1}{2} u_i(\xi) = 2\pi \int_{\overline{S}} u_{ij}^*(\xi, x) f_j(x) r(x)\, d\overline{S}(x) - 2\pi \int_{\overline{S}} f_{ij}^*(\xi, x) u_j(x) r(x)\, d\overline{S}(x), \tag{7}$$

where the subscripts i and j take the values r, z, $u_{ij}^*(\xi, x)$, $f_{ij}^*(\xi, x)$ are the kernel functions

$$u_{rr}^*(\xi, x) = \alpha\left((3-4\nu)Q_{+1/2}(\gamma) + \frac{\overline{Z}^2}{R\,r}\frac{dQ_{+1/2}}{d\gamma}\right),\ u_{rz}^*(\xi, x) = \frac{\alpha\overline{Z}}{r}\left(\frac{Q_{+1/2}(\gamma)}{2} - \left(\gamma - \frac{r}{R}\right)\frac{dQ_{+1/2}}{d\gamma}\right),$$

$$u_{zr}^*(\xi, x) = -\frac{\alpha\overline{Z}}{r}\left(\frac{Q_{-1/2}(\gamma)}{2} + \left(\gamma - \frac{r}{R}\right)\frac{dQ_{-1/2}}{d\gamma}\right),\ u_{zz}^*(\xi, x) = \alpha\left((3-4\nu)Q_{-1/2}(\gamma) - \frac{\overline{Z}^2}{R\,r}\frac{dQ_{-1/2}}{d\gamma}\right),$$

$$p_{rr}^*(\xi, x) = \frac{2\mu}{1-2\nu}\left\{\left[(1-\nu)\frac{\partial u_{rr}^*}{\partial r} + \nu\left(\frac{u_{rr}^*}{r} + \frac{\partial u_{rz}^*}{\partial z}\right)\right] n_r + \mu\left(\frac{\partial u_{rr}^*}{\partial z} + \frac{\partial u_{rz}^*}{\partial r}\right) n_z\right\},$$

$$p^*_{rz}(\xi,x)=\frac{2\mu}{1-2\nu}\left\{\left[(1-\nu)\frac{\partial u^*_{rz}}{\partial z}+\nu\left(\frac{u^*_{rr}}{r}+\frac{\partial u^*_{rr}}{\partial r}\right)\right]n_z+\mu\left(\frac{\partial u^*_{rr}}{\partial z}+\frac{\partial u^*_{rz}}{\partial r}\right)n_r\right\},$$

$$p^*_{zr}(\xi,x)=\frac{2\mu}{1-2\nu}\left\{\left[(1-\nu)\frac{\partial u^*_{zr}}{\partial r}+\nu\left(\frac{u^*_{zr}}{r}+\frac{\partial u^*_{zz}}{\partial z}\right)\right]n_r+\mu\left(\frac{\partial u^*_{zr}}{\partial z}+\frac{\partial u^*_{zz}}{\partial r}\right)n_z\right\},$$

$$p^*_{zz}(\xi,x)=\frac{2\mu}{1-2\nu}\left\{\left[(1-\nu)\frac{\partial u^*_{zz}}{\partial z}+\nu\left(\frac{u^*_{zr}}{r}+\frac{\partial u^*_{zr}}{\partial r}\right)\right]n_z+\mu\left(\frac{\partial u^*_{zr}}{\partial z}+\frac{\partial u^*_{zz}}{\partial r}\right)n_r\right\}. \quad (8)$$

Here, $R=r(\xi)$, $Z=z(\xi)$, $r=r(x)$, $z=z(x)$ are the cylindrical coordinates of the points ξ and x, $\overline{Z}=Z-z$, $\alpha=\frac{1}{16\pi^2(1-\nu)\mu\sqrt{R\,r}}$, $\gamma=1+\frac{\overline{Z}^2+(R-r)^2}{2\,R\,r}$, n_r and n_z are the components of the vector of the outer normal to the boundary $\overline{S}$. The Legendre functions $Q_{+1/2}(\gamma)$, $Q_{-1/2}(\gamma)$ and their derivatives can be represented in terms of complete elliptic integrals of the first and second kinds as

$$Q_{+1/2}(\gamma)=\gamma\,k\,K(m)-\frac{2}{k}E(m),\quad \frac{dQ_{+1/2}}{d\gamma}=\frac{k}{2}\left[K(m)-\frac{\gamma}{\gamma-1}E(m)\right],$$

$$Q_{-1/2}(\gamma)=k\,K(m),\quad \frac{dQ_{-1/2}}{d\gamma}=-\frac{k}{2}\frac{1}{\gamma-1}E(m), \quad (9)$$

where $K(m)$ and $E(m)$ are first- and second-kind complete elliptic integrals respectively, $m=\frac{2}{1+\gamma}$, $k=\sqrt{m}$.

To solve the boundary integral equation (7), we divide the boundary $\overline{S}$ into $N=n_1+n_2+n_3$ straight boundary elements as follows: $e_1,...,e_{n_1}$ on the boundary $\overline{S}_1$, $e_{n_1+1},...,e_{n_1+n_2}$ on the boundary $\overline{S}_2$, and $e_{n_1+n_2+1},...,e_N$ on the boundary $\overline{S}_3$. Assuming a constant approximation of displacements u_i and surface stresses f_i on the boundary element, in view of the boundary conditions (4) – (6), we obtain the following system of linear algebraic equations, corresponding to equation (7):

$$\frac{1}{2}u_i^{(k)}+2\pi\sum_{l=1}^{n_1+n_2}u_i^{(l)}\int_{e_l}f^*_{ij}(\xi_k,x)r(x)\,d\overline{S}(x)-2\pi\sum_{l=n_1+n_2+1}^{N}f_i^{(l)}\int_{e_l}u^*_{ij}(\xi_k,x)r(x)\,d\overline{S}(x)=$$

$$=2\pi\sum_{l=1}^{n_1}f_i^{*(l)}\int_{e_l}u^*_{ij}(\xi_k,x)r(x)\,d\overline{S}(x),\quad k=1,...,n_1+n_2,$$

$$2\pi\sum_{l=1}^{n_1+n_2}u_i^{(l)}\int_{e_l}f^*_{ij}(\xi_k,x)r(x)\,d\overline{S}(x)-2\pi\sum_{l=n_1+n_2+1}^{N}f_i^{(l)}\int_{e_l}u^*_{ij}(\xi_k,x)r(x)\,d\overline{S}(x)=$$

$$=2\pi\sum_{l=1}^{n_1}f_i^{*(l)}\int_{e_l}u^*_{ij}(\xi_k,x)r(x)\,d\overline{S}(x),\quad k=n_1+n_2+1,...,N. \quad (10)$$

Here, ξ_k is the node located in the middle of the boundary element e_k, $u_i^{(k)}$ and $f_i^{(k)}$ are the values of displacements and surface stresses on the element e_k. The values $u_i^{(k)}$ on the boundaries $\overline{S}_1$ and $\overline{S}_2$ and the values $f_i^{(k)}$ on the boundary $\overline{S}_3$ are the unknowns in system (10). The solution of the system will determine the displacements in the domain $\overline{V}$,

$$u_i(\xi)=2\pi\sum_{l=1}^{n_1}f_i^{*(l)}\int_{e_l}u^*_{ij}(\xi_k,x)r(x)\,d\overline{S}(x)+2\pi\sum_{l=n_1+n_2+1}^{N}f_i^{(l)}\int_{e_l}u^*_{ij}(\xi_k,x)r(x)\,d\overline{S}(x)-$$

$$-2\pi \sum_{l=1}^{n_1+n_2} u_i^{(l)} \int_{e_l} f_{ij}^*(\xi_k, x) r(x) d\bar{S}(x). \quad (11)$$

The continuous form of the solution (11) allows the stress distribution in the domain $\bar{V}$ to be determined according to equations (2) and (3).

The developed algorithm enables us to identify the shape of a human cornea and the distribution of stresses inside it at specified parameters. The solution is obtained in the form of a smooth function, this being essentially advantageous for its analysis over the finite element solution.

At the next stage of the study, the constructed algorithm can be applied to the calculation of the SSS in the cornea after laser vision correction surgery, its result being identification of the cornea shape after the surgery.

SOFTWARE IMPLEMENTATION

The discussed solution algorithm is implemented in the form of software written in C++ with the use of concurrent programming technologies. The program window is shown in Fig. 2. The finite element integrals involved in equations (10) and (11) are calculated numerically with the use of the simple Gaussian quadrature, except for the integrals over the elements containing points of singularity of elliptic integrals. The computation of singular integrals employs an adaptive numerical integration algorithm taking into account the known coordinates of singular points.

The GSL library [24] and the Boost library collection [25] are used in the program, the OpenMP standard [26] being used for the implementation of parallel computations. The program was tried out on a test problem having an analytical solution.

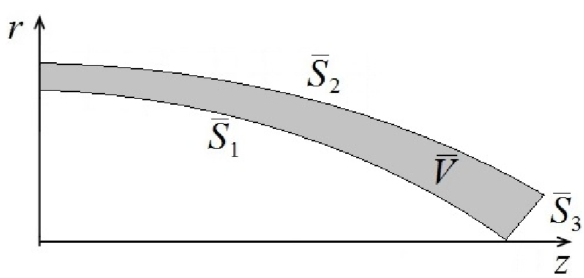

FIGURE 1. The solution domain $\bar{V}$

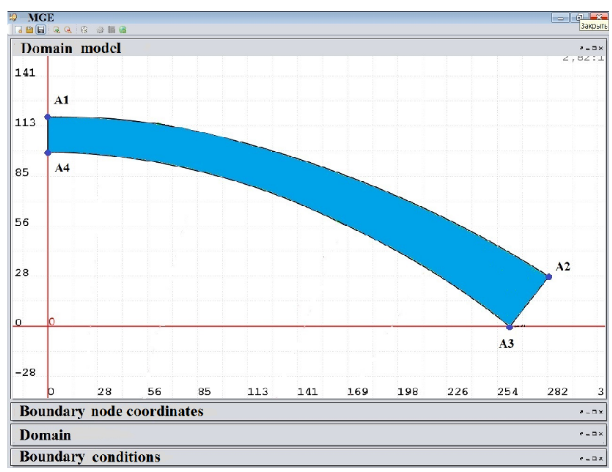

FIGURE 2. The window of the program for cornea SSS calculation

CONCLUSION

A procedure for solving an elastostatics problem in the axisymmetric statement has been developed. As applied to ophthalmological problems, the results of the study will allow the stress-strain state of the human cornea to be studied at specified geometrical and mechanical parameters. In our further research we plan to compare the calculation results with the available clinical evidence and to develop prediction techniques.

REFERENCES

1. E. P. Tarutta and N. G. Kvaratskhelija, R. F. Patent No. 2386418 (2010).
2. Statistics and Data. Hyperopia, National Eye Institute, USA, see https://nei.nih.gov/eyedata/hyperopia.

3. E. Maul, S. Barroso, S. R. Munoz, R. D. Sperduto, and L. B. Ellwein, Am. J. Ophthalmol. **129**, 445–454 (2000).
4. J. Zhao, X. Pan, R. Sui, S. R. Munoz, R. D. Sperduto, and L. B. Ellwein, Am. J. Ophthalmol. **129**, 427–435 (2000).
5. M. He, J. Zeng, Y. Liu, J. Xu, G. P. Pokharel, and L. B. Ellwein, Invest. Ophthalmol. Vis. Sci. **45**, 793–799 (2004).
6. A. Sawada, A. Tomidokoro, M. Araie, A. Iwase, and T. Yamamoto, Ophthalmology **115**, 363–370 (2008).
7. R. P. Vito and P. H. Carnell, Refract. Corneal Surg. **8**, 146–151 (1992).
8. J. Al-Sukhun, C. Lindqvist, and R. Kontio, J. R. Soc. Interface **3**, 255–262 (2006).
9. V. Alastrué, B. Calvo, E. Peña, and M. Doblaré, J. Biomech. Eng. **128**, 150 (2006).
10. M. L. Kochina and V. G. Kalimanov, Clinical Informatics and Telemedicine **5**, 26–30 (2009).
11. E.N. Iomdina and M.V. Poloz, Russian J. of Biomechanics **14,** 7–18 (2010).
12. S. M. Bauer, L. A. Venatovskaya, D. V. Franus, and L. A. Fedotova, Russian J. of Biomechanics **19,** 136–143 (2015).
13. S. M. Bauer and E. B. Voronkova, Vestnik St. Petersburg University: Ser. 1. Mathematics. Mechanics. Astronomy **1**, 438–458 (2014).
14. E. V. Krakovskaya, Vestnik St. Petersburg University: Ser. 1. Mathematics. Mechanics. Astronomy **2**, 129–132 (2008).
15. A. L. Kazakov and L. F. Spevak, Appl. Math. Model. **37**, 6918–6928 (2013).
16. V. P. Fedotov, L. F. Spevak, and O. A. Nefedova, Software & Systems **4**, 178–183 (2014).
17. A. L. Kazakov and L. F. Spevak, Appl. Math. Model. **40**, 1333–1343 (2016).
18. L. F. Spevak and O. A. Nefedova, "Solving a two-dimensional nonlinear heat conduction equation with degeneration by the boundary element method with the application of the dual reciprocity method," in *Mechanics, Resource and Diagnostics of Materials and Structures*-2016, AIP Conference Proceedings 1785, edited by Eduard S. Gorkunov *et al*. (American Institute of Physics, Melville, NY, 2016), p. 040077.
19. L. F. Spevak and O. A. Nefedova, "Solving a two-dimensional nonlinear heat conduction equation with nonzero boundary conditions by the boundary element method," in *Mechanics, Resource and Diagnostics of Materials and Structures*-2017, AIP Conference Proceedings 1915, edited by Eduard S. Gorkunov *et al*. (American Institute of Physics, Melville, NY, 2017), p. 040055.
20. A.L. Kazakov, L.F. Spevak, and O.A. Nefedova, "Solving a two-dimensional problem of heat wave initiation by a boundary condition specified on a movable manifold," in *Mathematical Problems of Continuum Mechanics*, IOP Conf. Series 1268 (Institute of Physics, London, UK, 2019), p. 012031.
21. V. P. Fedotov and L. F. Spevak, Eng. Anal. Boundary Elem. **32**, 883–888 (2008).
22. L. F. Spevak and O. A. Nefedova, "Parallel technology for solving the poisson equation in axisymmetric domains by the boundary element method," in *Mechanics, Resource and Diagnostics of Materials and Structures*-2018, AIP Conference Proceedings 2053, edited by Eduard S. Gorkunov *et al*. (American Institute of Physics, Melville, NY, 2018), p. 030070.
23. C. A. Brebbia, J. F. C. Telles, and L. C. Wrobel, *Boundary Element Techniques. Theory and Applications in Engineering* (Springer-Verlag, Berlin, Neidelberg, New-York, Tokyo, 1984), pp. 224–230.
24. GSL-GNU Scientific Library, see http://www.gnu.org/software/gsl/.
25. Boost C++ Libraries, see http://www.boost.org.
26. OpenMP, see http://www.openmp.org.